Calpain Inhibition Preserves Talin and Attenuates Right Heart Failure in Acute Pulmonary Hypertension

Hasan A. Ahmad[1], Li Lu[1], Shuyu Ye[1], Gregory G. Schwartz[1], and Clifford R. Greyson[1]

[1]Cardiology Section, Veterans Affairs Medical Center and the University of Colorado, Denver, Colorado

Right heart failure from right ventricular (RV) pressure overload is a major cause of morbidity and mortality, but its mechanism is incompletely understood. We tested the hypothesis that right heart failure during 4 hours of RV pressure overload is associated with alterations of the focal adhesion protein talin, and that the inhibition of calpain attenuates RV dysfunction and preserves RV talin. Anesthetized open-chest pigs treated with the calpain inhibitor MDL-28170 ($n = 20$) or inactive vehicle ($n = 23$) underwent 4 hours of RV pressure overload by pulmonary artery constriction (initial RV systolic pressure, 64 ± 1 and 66 ± 1 mm Hg in MDL-28170 and vehicle-treated pigs, respectively). Progressive RV contractile dysfunction was attenuated by MDL-28170: after 4 hours of RV pressure overload, RV systolic pressure was 44 ± 4 mm Hg versus 49 ± 6 mm Hg ($P = 0.011$), and RV stroke work was 72 ± 5% of baseline versus 90 ± 5% of baseline, ($P = 0.027$), in vehicle-treated versus MDL-28170–treated pigs, respectively. MDL-28170 reduced the incidence of hemodynamic instability (death or systolic blood pressure of < 85 mm Hg) by 46% ($P = 0.013$). RV pressure overload disrupted talin organization. MDL-28170 preserved talin abundance in the RV free wall ($P = 0.039$), and talin abundance correlated with the maintenance of RV free wall stroke work ($r = 0.58$, $P = 0.0039$). α-actinin and vinculin showed similar changes according to immunohistology. Right heart failure from acute RV pressure overload is associated with reduced talin abundance and disrupted talin organization. Calpain inhibition preserves the abundance and organization of talin and RV function. Calpain inhibition may offer clinical utility in treating acute cor pulmonale.

Keywords: right ventricular dysfunction; pulmonary hypertension; calpain; talin; heart failure

CLINICAL RELEVANCE

Right heart failure from acute right ventricular pressure overload is a major cause of morbidity and mortality, but its mechanism is incompletely understood, and no specific therapy is available for right heart failure in this setting. In our study, acute right ventricular pressure overload caused right heart failure and disruption of the focal adhesion protein talin. Talin disruption and right ventricular contractile dysfunction were tightly correlated. Vinculin and α-actinin, other important adhesion proteins, were also altered by right ventricular pressure overload. Calpain inhibition attenuated the severity of right heart failure and preserved the organization of talin, vinculin, and α-actinin. Calpain inhibition may offer clinical utility in mitigating the severity of acute cor pulmonale.

Right ventricular (RV) failure from acute right ventricular pressure overload (RVPO) is a major cause of morbidity and mortality in conditions such as pulmonary embolism and hypoxic pulmonary vasoconstriction, and in the early period after cardiopulmonary bypass or cardiac transplantation (1, 2). In the past, the conventional understanding of the pathophysiology of acute RV failure attributed it either to RV ischemia or to abnormal loading conditions during RVPO. However, we and others (3–5) previously demonstrated that the pathophysiology is more complex: a brief period of RVPO without RV ischemia results in intrinsic RV contractile dysfunction that persists beyond the period of RVPO itself, despite the restoration of normal loading conditions. Thus, the mechanism of intrinsic contractile dysfunction provoked by RVPO remains uncertain.

Current clinical treatments for acute RV failure from RVPO depend almost exclusively on inotropic therapy or measures intended to relieve the underlying RVPO, such as thrombolysis, pulmonary thromboendarterectomy, and pulmonary vasodilators. These measures often result in serious complications, do not fully mitigate the high mortality, and do not directly address the mechanisms of intrinsic RV contractile dysfunction. A treatment that addresses and mitigates intrinsic contractile dysfunction in RVPO might offer considerable clinical utility.

Substantial evidence indicates that the calcium-activated cysteine protease calpain plays a role in the pathogenesis of muscle dysfunction in multiple settings (6). We recently reported that the narrow-spectrum calpain inhibitor MDL-28170 mitigated the severity of RV contractile dysfunction when normal loading conditions were restored after 90 minutes of RVPO (7). In that study, however, we found no effect of MDL-28710 on some of the most widely recognized calpain substrates, including troponin, desmin, and spectrin, leaving the mechanism of hemodynamic benefit uncertain. Moreover, clinically significant RV failure from RVPO usually occurs *during* the period of pressure overload, and not after its relief.

Calpain plays an important role in modifying focal adhesions, protein complexes that participate in intercellular attachment and mechanical signal transduction. In particular, talin is a key protein that links integrin to the cytoskeleton, is highly sensitive to calpain, and plays a central role in focal adhesion dynamics (8). The present study was designed to explore whether modification of talin is associated with the development of RV failure from RVPO, and to test the hypothesis that the salutary effects of calpain inhibition with MDL-28170 are evident *during*

(*Received in original form August 16, 2011 and in final form May 2, 2012*)

H.A.A., G.G.S., and C.R.G. (principal investigator) were responsible for the conception and design of the experiment. H.A.A., L.L., and C.R.G. were responsible for the execution of animal experiments. H.A.A., S.Y., and C.R.G. were responsible for biochemical and histological analyses. H.A.A., G.G.S., and C.R.G. were responsible for the analysis and interpretation of data. H.A.A. and C.R.G. were responsible for drafting the manuscript. H.A.A., L.L., S.Y., G.G.S., and C.R.G. were responsible for the revision, review, and final approval of the manuscript.

This work was supported by the Department of Veterans Affairs Medical Research Service, by National Heart, Lung, and Blood Institute grants HL076072 (H.A.A.), HL68606 (C.R.G.), and HL49444 (G.G.S.) from the National Institutes of Health, and by a research grant from Bayer Schering Pharma (C.R.G.).

Correspondence and requests for reprints should be addressed to Clifford R. Greyson, M.D., Cardiology Section, Veterans Affairs Medical Center, 1055 Clermont Street, Cardiology 111B, Denver, CO 80220. E-mail: Clifford.Greyson@UCDenver.edu

This article has an online supplement, which is accessible from this issue's table of contents at www.atsjournals.org

Am J Respir Cell Mol Biol Vol 47, Iss. 3, pp 379–386, Sep 2012
Published 2012 by the American Thoracic Society
Originally Published in Press as DOI: 10.1165/rcmb.2011-0286OC on May 10, 2012
Internet address: www.atsjournals.org

sustained RVPO and result in clinically relevant improvements of hemodynamics.

Some of the results of these studies were previously reported in the form of abstracts (9, 10).

MATERIALS AND METHODS

See the online supplement for additional details.

Experimental Preparation and Experimental Protocol

The experimental preparation was similar to that previously described by this laboratory (4). Forty-three juvenile domestic farm pigs, instrumented as illustrated in Figure 1, were assigned to receive either inactive vehicle (1% DMSO/PBS vehicle, pH 7.40) or the narrow-spectrum calpain inhibitor MDL-28170 (10 μM per liter in vehicle; CalBiochem, Billerica, MA), via infusion into the right coronary artery. Treatment assignment was blinded during the experimental protocol by randomly selecting coded vials of solution that had been prepared in advance by an investigator not directly involved in the animal experiments.

The experimental protocol is schematized in Figure 2. After baseline hemodynamic and sonomicrometry measurements, vehicle or MDL-28170 infusion was initiated at 10% of right coronary artery flow (measured with an ultrasonic flow probe) to achieve 1 μM MDL-28170 (K_i for calpain, ~8 nM) (11) and 0.1% DMSO coronary arterial concentration, and continued throughout the remainder of the experiment. Measurements were repeated after 20 minutes to determine any effects of treatment before RVPO. Next, the pulmonary artery occluder was gradually constricted over 5 to 10 minutes to obtain maximum RV systolic pressure (the point where further pulmonary artery constriction caused RV systolic pressure to decline). This degree of constriction was fixed for the duration of RVPO. Additional sets of hemodynamic data were obtained early (10–20 min) and later (230–240 min) after beginning pulmonary artery constriction. The snare was then released, recovery measurements were obtained 10–20 minutes later, and the pigs were killed.

Hemodynamic Data Analysis

Global RV systolic function during acute RVPO was assessed using peak developed RV pressure, cardiac output, and global RV stroke work. Regional RV systolic function was assessed using sonomicrometry and regional Frank–Starling relations, as previously described (3, 4).

Polyacrylamide Gel Electrophoresis and Western Immunoblotting

Standard one-dimensional electrophoresis and immunoblotting were used to identify proteins potentially related to the development of RV dysfunction, as previously described (7).

Immunohistology

Fifteen additional pigs were subjected to 2 hours of sham pressure overload ($n = 4$), or 2 hours of RVPO with vehicle ($n = 7$) or MDL-28170 treatment ($n = 4$) for the investigation of changes occurring in RV myocardial structure early in the development of RV dysfunction, before significant hemodynamic deterioration occurred. In four of the vehicle-treated RVPO pigs, drill biopsies of the RV free wall were obtained under baseline conditions before beginning RVPO as previously described (12). Tissue was cryosectioned, immunolabeled for talin, α-actinin, or vinculin, and examined via digital deconvolution microscopy.

Statistical Analysis

Measurements are reported as means ± standard errors of the mean. Significant differences were identified with repeated-measures ANOVA performed on raw measurements or on log-transformed data (to eliminate differences attributable to scaling, or to stabilize variance). When the P for trend was ≤ 0.1 (i.e., suggestive of a true effect) (13), individual contrasts were performed using unadjusted unpaired t tests. The effect of treatment on hemodynamic stability was analyzed according to the Fisher exact test. The relationship between protein abundance and function was determined by simple linear regression.

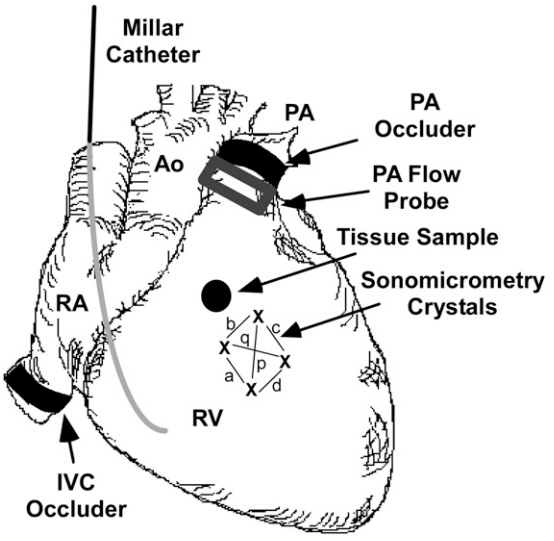

Figure 1. Instrumentation of the heart. A solid-state micromanometer catheter was introduced into the right ventricle (RV) via an internal jugular vein. An array of four sonomicrometry crystals (indicated by *x*) was inserted into the mid-RV free wall and used to calculate wall area (*see* online supplement). Chord lengths used to calculate area are designated by *a*, *b*, *c*, *d*, *p*, and *q*. Ultrasonic transit-time flow probes were placed around the main pulmonary artery for the measurement of cardiac output, and around the proximal right coronary artery for the measurement of coronary artery flow. An umbilical tape snare was placed around the pulmonary artery to produce right ventricular pressure overload (RVPO), and a hydraulic occluder was placed around the inferior vena cava to alter preload. In addition to the instrumentation illustrated here, a micromanometer catheter was inserted into the left ventricle via apical puncture, pacing wires were affixed to the left atrial appendage, and a 26-gauge catheter was inserted into the proximal right coronary artery. A lead II electrocardiogram was recorded from needle electrodes placed subcutaneously in the four limbs. Ao, aorta; RA, right atrium; PA, pulmonary artery; RV, right ventricle; IVC, inferior vena cava.

RESULTS

Forty-three pigs were randomized to vehicle ($n = 23$) or MDL-28170 ($n = 20$). Table 1 (*see also* Figure E1 in the online supplement) shows hemodynamic data for the two groups. Baseline RV systolic pressure was the same in vehicle-treated (36 ± 1 mm Hg) and MDL-28170–treated (38 ± 1 mm Hg) pigs. Neither the infusion of MDL-28170 nor of vehicle exerted any significant effects on hemodynamics before RVPO. RV systolic pressure increased to a similar extent in both groups at the onset of RVPO (vehicle, 62 ± 1 mm Hg; MDL-28170, 64 ± 1 mm Hg). Fifteen additional pigs were used for the immunohistology studies. Hemodynamics at baseline and during RVPO were similar in these pigs.

MDL-28170 Preserved RV Global Function and Reduced the Frequency of Hemodynamic Instability

During RVPO, fewer pigs in the MDL-28170 group than in the vehicle group developed hemodynamic instability (defined as systolic blood pressure < 85 mm Hg or hemodynamic collapse, occurring in 19 of 23 vehicle pigs, versus nine of 20 MDL-28170 pigs; $P = 0.013$ by the Fisher exact test). Eight of these pigs (five vehicle-treated and three MDL-28170–treated) died before the end of RVPO. The data for these pigs are not included in the "RVPO 4 hour" or "Recovery" columns of Table 1, and were not used in the statistical analysis of contractile function. RV pulsus alternans (defined as an alternation in RV systolic pressure of at

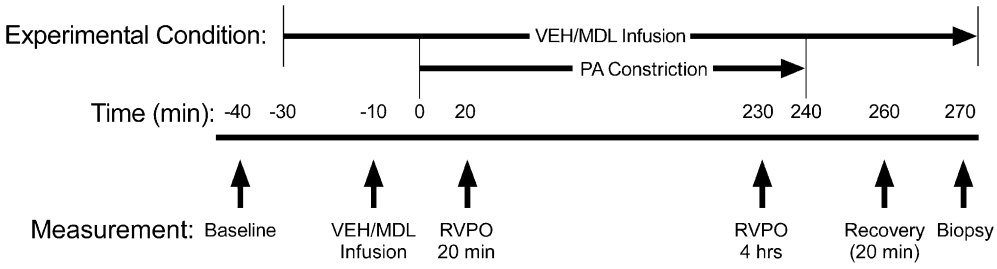

Figure 2. Experimental protocol. *Vertical arrows* indicate the approximate time at which hemodynamic measurements were obtained. Treatment assignment was blinded during the experimental protocol by randomly selecting coded vials of solutions of vehicle (VEH) or MDL-28170 (MDL) that had been prepared in advance by an investigator not directly involved in the animal experiments. After baseline measurements of hemodynamics and RV function, an infusion of either inactive vehicle or MDL-28170 was begun and a second set of measurements of hemodynamics and RV function was repeated 20 minutes later to determine any effects of treatment in the absence of RVPO (designated *Infusion*). Next, the pulmonary artery umbilical tape snare was gradually constricted for 5–10 minutes to obtain maximum RV systolic pressure (the point at which additional pulmonary artery constriction resulted in a decline in RV systolic pressure). This degree of pulmonary artery constriction was fixed for the ensuing 4 hours to simulate clinical conditions of increased pulmonary vascular resistance. Additional sets of hemodynamic data were obtained early (10–20 min, designated *RVPO 20 min*) and later (230–240 min, designated *RVPO 4 hrs*) after beginning pulmonary artery constriction. In the 35 pigs surviving until the end of the 4 hours of RVPO, the snare was released and "recovery" measurements were obtained 10–20 minutes later. In approximately half of the pigs, the heart was arrested with 10% KCl, and the central RV free wall was excised and frozen on a liquid nitrogen–cooled steel mortar for later analysis. Tissue from pigs that died before the end of the protocol was not analyzed, because low perfusion pressure in those pigs could have caused antemortem ischemia and resulted in nonspecific protein degradation.

least 1 mm Hg, lasting at least 10 beats and not associated with arrhythmia) developed in four MDL-28170 pigs versus 12 vehicle pigs (Figure 3; $P = 0.056$ by the Fisher exact test).

Of pigs surviving through 4 hours of RVPO, MDL-28170–treated pigs maintained significantly higher RV pressure (MDL-28170–treated versus vehicle-treated, 49 ± 1 mm Hg versus 44 ± 1 mm Hg, respectively; $P = 0.011$) and cardiac output (MDL-28170–treated versus vehicle-treated, 65% ± 4% versus 52% ± 3% of baseline, respectively; $P = 0.015$) at the end of the RVPO period. RV stroke work was the same in both groups at baseline, and increased to a similar extent at 20 minutes of RVPO. Although RV stroke work declined during sustained RVPO in both groups, at 4 hours of RVPO, MDL-28170–treated animals generated significantly higher stroke work compared with vehicle-treated pigs (90% ± 5% versus 72% ± 5% of baseline in the MDL-28170 versus vehicle groups, respectively; $P = 0.021$). At the recovery measurement (20 min after the release of RVPO), RV stroke work was not significantly different between groups.

MDL-28170 Preserved RV Regional Free Wall Function in Parallel with RV Global Function

Regional RV free wall indices of contractile function paralleled measurements of global RV function (Table 2 and Figure E2): at the end of 4 hours of RVPO, RV free wall external work was 73% ± 5% versus 56% ± 7% of baseline in the MDL-28170 versus vehicle groups, respectively ($P = 0.020$). At the recovery measurement, the slope of the regional Frank–Starling relation was 89% ± 7% of baseline in MDL-28170 pigs, compared with only 68% ± 6% of baseline in vehicle pigs ($P = 0.020$), indicating that regional RV free wall contractile function was better preserved in MDL-28170 pigs. MDL-28170 pigs tended to

TABLE 1. GLOBAL HEMODYNAMICS

	Baseline	Infusion	RVPO (20 min)	RVPO (4 h)	Recovery (20 min)
Heart rate (bpm)					
Vehicle	129 ± 2	128 ± 2	129 ± 2	129 ± 2	124 ± 4
MDL-28170	128 ± 2	128 ± 2	128 ± 2	128 ± 3	128 ± 3
LV systolic pressure (mm Hg)					
Vehicle	102 ± 2	103 ± 3	95 ± 3	83 ± 4	86 ± 5
MDL-28170	105 ± 3	103 ± 3	96 ± 3	90 ± 4*	91 ± 3
RV systolic pressure (mm Hg): overall $P = 0.047$ for vehicle versus MDL-28170					
Vehicle	36 ± 1	36 ± 1	62 ± 1	44 ± 1	35 ± 2
MDL-28170	38 ± 1	37 ± 1	64 ± 1	49 ± 1†	33 ± 1
Cardiac output (L/minute): overall $P = 0.059$ for vehicle versus MDL-28170					
Vehicle	4.8 ± 0.2	4.5 ± 0.2	3.4 ± 0.2	2.5 ± 0.2	2.7 ± 0.2
MDL-28170	4.2 ± 0.2#	4.3 ± 0.2	3.4 ± 0.2‡	2.7 ± 0.2§	2.7 ± 0.2¶
Global RV stroke work (L · mm Hg/beat): overall $P = 0.085$ for vehicle versus MDL-28170					
Vehicle	1.09 ± 0.07	1.04 ± 0.08	1.45 ± 0.12	0.77 ± 0.07	0.68 ± 0.06
MDL-28170	1.01 ± 0.06	1.00 ± 0.07	1.44 ± 0.08	0.91 ± 0.08#	0.60 ± 0.05

Definition of abbreviations: bpm, beats per minute; LV, left ventricular; RV, right ventricular; RVPO, right ventricular pressure overload.

All values represent means ± SEM.

*Nineteen of 23 vehicle pigs versus nine of 20 MDL-28170 pigs developed hemodynamic instability (defined as death or systolic blood pressure < 85 mm Hg, $P = 0.013$ by the Fisher exact test).

† For RV systolic pressure, $P = 0.011$ for vehicle versus MDL-28170.

‡ For cardiac output normalized to baseline value, $P = 0.078$.

§ For cardiac output normalized to baseline value, $P = 0.015$.

¶ For cardiac output normalized to baseline value, $P = 0.042$.

For global RV stroke work normalized to baseline value, $P = 0.021$ for VEH versus MDL-28170. For un-normalized cardiac output, $P = 0.040$ for VEH versus MDL.

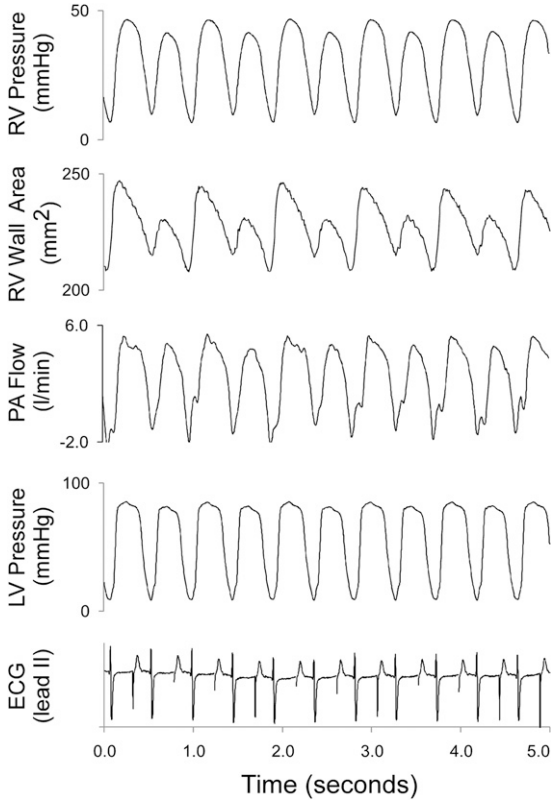

Figure 3. Examples of hemodynamic data obtained in a pig treated with inert vehicle that developed RV pulsus alternans near the end of 4 hours of RVPO. Prominent alterations of RV pressure, RV free wall contraction, and pulmonary artery (PA) flow occurred. The minimal concurrent alternation of left ventricular (LV) pressure was likely attributable to interventricular interactions. The electrocardiogram (ECG) indicates atrial paced rhythm. Treatment with MDL-28170, compared with vehicle, reduced the incidence of RV pulsus alternans (52% versus 20%, respectively; $P = 0.056$).

demonstrate lower regional Frank–Starling relation dimension axis intercepts (also indicating less dysfunction) and greater regional external work adjusted for preload compared with vehicle pigs, although these differences did not reach statistical significance.

MDL-28170 Preserved Talin Abundance, and Talin Abundance Was Related to RV Function

Western immunoblots for spectrin, desmin, troponin-I, and sarco/endoplasmic reticulum Ca^{2+}-ATPase showed low levels of protein degradation in both groups, similar to what we and others previously reported. However, no significant differences between MDL-28170–treated and vehicle-treated pigs could be detected in any of those proteins (immunoblots not shown). These are similar to the results we reported for pigs subjected to only 90 minutes of RVPO (7). We next performed Western immunoblotting for talin. Figure 4 shows a representative Western blot immunostained for talin and α-tubulin. MDL-28170 preserved talin abundance (normalized talin/α-tubulin ratio, 0.97 ± 0.07 versus 0.80 ± 0.04, with MDL-28170 21% higher; $P = 0.039$). Figure 5 shows that talin abundance at the end of 4 hours of RVPO bore a highly significant relationship to the preservation of external regional RV stroke work at that time point ($r = 0.58$, $P = 0.0039$). A similar relationship was evident between talin abundance and global RV stroke work ($r = 0.47$, $P = 0.026$). When both MDL-28170 treatment and talin abundance were incorporated into a two-way ANOVA, the main effect of talin remained significant ($P = 0.0088$), but the effect of MDL-28170 treatment became nonsignificant; that is, the beneficial effect of MDL-28170 treatment was highly correlated with its effect on the preservation of talin abundance, and thus MDL-28170 did not appear to contribute to the preservation of stroke work through mechanisms unrelated to its effect on talin abundance.

A trend toward the preservation of α-actinin by MDL-28170 (9% higher abundance) was evident, but this did not reach statistical significance ($P = 0.13$). No difference in vinculin was apparent from Western immunoblotting (Figure 4).

RVPO Altered the Organization of Talin, α-Actinin, and Vinculin According to Immunohistology

Figure 6 shows representative 0.5-μm optical sections under baseline conditions, in the same pigs after 2 hours of RVPO, in separate sham pigs not subjected to RVPO but undergoing identical instrumentation and the same 2 hours of anesthesia, and in pigs subjected to RVPO after pretreatment with MDL-28170. Under baseline conditions, talin (shown in *red*) has a discrete distribution, localized predominantly along the cell surface. After 2 hours of RVPO, disruption of the regular distribution of talin occurred, along with scattered areas of diffusion and a blurring of the talin signal. This was not seen in the sham experiments, and was attenuated by pretreatment with MDL-28170. A three-dimensional reconstruction of one of the experiments is shown in Figure 7 (*see also* the video files in the online supplement). Under baseline conditions, talin exhibited a rib-like structure (*see* "Talin Structure at Baseline.mov" in the online supplement). This rib-like structure was disrupted after 2 hours of RVPO, consistent with the thin-section appearance demonstrated in Figure 5 (*see* "Talin Structure after RVPO.mov" in the online supplement). The blurring (*green arrow*) and loss (*white arrow*) of talin signal, as shown for experiment 2 in Figure 5, are indicated at the corresponding locations on the three-dimensional reconstruction. In composite, the talin abundance and immunohistology results indicate that RVPO adversely affected both the quantity and organization of talin. Similar findings were apparent for α-actinin (Figure E3) and vinculin (Figure E4).

DISCUSSION

This investigation produced two key findings: the alteration of talin structure is strongly associated with the development of RV dysfunction from acute RVPO, and the calpain inhibitor MDL-28170 attenuates the development of right heart failure during 4 hours of sustained RVPO. The difference was manifested by the maintenance of higher RV systolic pressure, higher cardiac output, higher RV stroke work, and better preservation of contractile indices derived from the regional Frank–Starling relation. Importantly, MDL-28170 prevented the development of hemodynamic instability compared with vehicle, and attenuated the development of RV pulsus alternans, which has been observed clinically in severe RVPO (14). Thus, calpain inhibition exerted a major salutary impact on clinically relevant measures of right heart failure during 4 hours of RVPO. The salutary effects of MDL-28170 on right heart function were accounted for statistically by preservation of the focal adhesion protein talin, as indicated by the strong correlation between talin abundance and RV function. Although correlation is not proof of causality, our immunohistology results are consistent with the known two-dimensional lattice structure of talin and other costameric proteins (15), and suggest that the structure of talin was altered by RVPO and preserved by MDL-28170. α-actinin, a major adhesion protein that is localized to the sarcomeric Z-disk and plays

TABLE 2. REGIONAL HEMODYNAMICS

	Baseline	Infusion	RVPO (20 min)	RVPO (4 h)	Recovery (20 min)
Regional external work (fraction of baseline): $P = 0.033$ for MDL-28170 versus vehicle					
Vehicle	1	0.98 ± 0.03	1.55 ± 0.13	0.56 ± 0.07	0.50 ± 0.06
MDL-28170	1	0.98 ± 0.04	1.67 ± 0.11	0.73 ± 0.05*	0.55 ± 0.04
End-diastolic area (fraction of baseline)					
Vehicle	1	1.00 ± 0.01	1.18 ± 0.04	1.05 ± 0.06	1.08 ± 0.06
MDL-28170	1	1.00 ± 0.02	1.19 ± 0.07	1.04 ± 0.05	1.00 ± 0.04
Regional Frank–Starling relation slope (fraction of baseline)					
Vehicle	1	1.01 ± 0.02			0.68 ± 0.06
MDL-28170	1	1.06 ± 0.05			0.89 ± 0.07†
Regional Frank–Starling Relation intercept (fraction of baseline)					
Vehicle	1	1.01 ± 0.01			1.18 ± 0.07
MDL-28170	1	1.02 ± 0.01			1.15 ± 0.04
Regional external work normalized to baseline at matched end-diastolic area					
Vehicle	1	0.98 ± 0.02			0.45 ± 0.12
MDL-28170	1	0.99 ± 0.03			0.55 ± 0.09

All values represent means ± SEM.

* $P = 0.020$ for vehicle pigs versus MDL-28170 pigs.

† For regional Frank–Starling slope normalized to baseline value, $P = 0.020$ for vehicle pigs versus MDL-28170 pigs. Indices derived from the Frank–Starling relation were not determined during RVPO because IVC occlusion during severe RVPO results in hemodynamic instability.

a key role in anchoring actin, and vinculin, another important adhesion protein, also showed evidence of changes in organization after RVPO.

We and others have shown that RV contractile dysfunction from acute RVPO can occur in the absence of detectable ischemia (3, 16, 17), and we previously reported that desmin, troponin-I, and spectrin (proteins that are reportedly degraded in some models of experimental ischemia/reperfusion) (18–24) are not degraded in our model of acute RVPO (7). In that study (7), we considered the possibility that we might have failed to detect the degradation of these proteins because of the relatively short period of RVPO. However, in the present study, we again found no evidence of significant degradation of these proteins, despite more prolonged RVPO and more severe RV dysfunction. This suggests that the degradation of those proteins is minor if it occurs at all, is unlikely to account for the functional differences we found, and that other calpain targets are more likely responsible for RV dysfunction in acute RVPO and are preserved by MDL-28170. The present findings also provide indirect evidence that ischemia is not causally related to the development of RV dysfunction in this model, since proteins commonly degraded during ischemia were unaffected in our model.

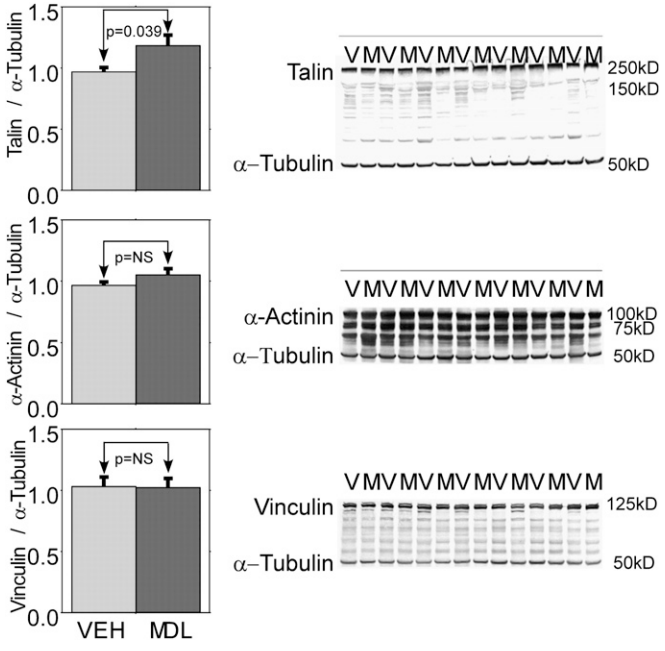

Figure 4. Summary results and representative examples of Western immunoblots probed for talin (*top*), α-actinin (*middle*), and vinculin (*below*) in RV myocardium obtained at the end of RVPO in pigs treated with vehicle (V) or the calpain inhibitor MDL-28170 (M). Band intensities of talin, α-actinin, vinculin, and α-tubulin were each normalized to the mean of a fiduciary set of four samples that were repeated on each gel; α-tubulin was used as a loading standard. The talin/α-tubulin ratio was 21% higher in pigs treated with MDL-28170 than in pigs treated with vehicle ($P = 0.039$). A trend toward a higher α-actinin/α-tubulin ratio (9%) in MDL-28170 pigs was evident, but this difference did not reach statistical significance ($P = 0.12$). No difference in vinculin/α-tubulin ratio was evident between the two groups.

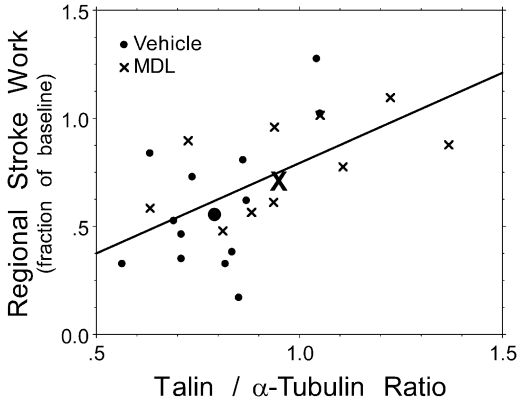

Figure 5. Function versus talin: relationship between talin abundance and preservation of regional external RV work at the end of RVPO. The preservation of regional external RV work was strongly dependent on the preservation of talin abundance ($r = 0.58$, $P = 0.0039$). A similar relationship existed between talin/α-tubulin ratio and global RV stroke work ($r = 0.47$, $P = 0.026$). The *large bold symbols* (*dots* for vehicle, and *X* for MDL-28170) show the mean values (centroids) for vehicle and MDL-28170 pigs, respectively.

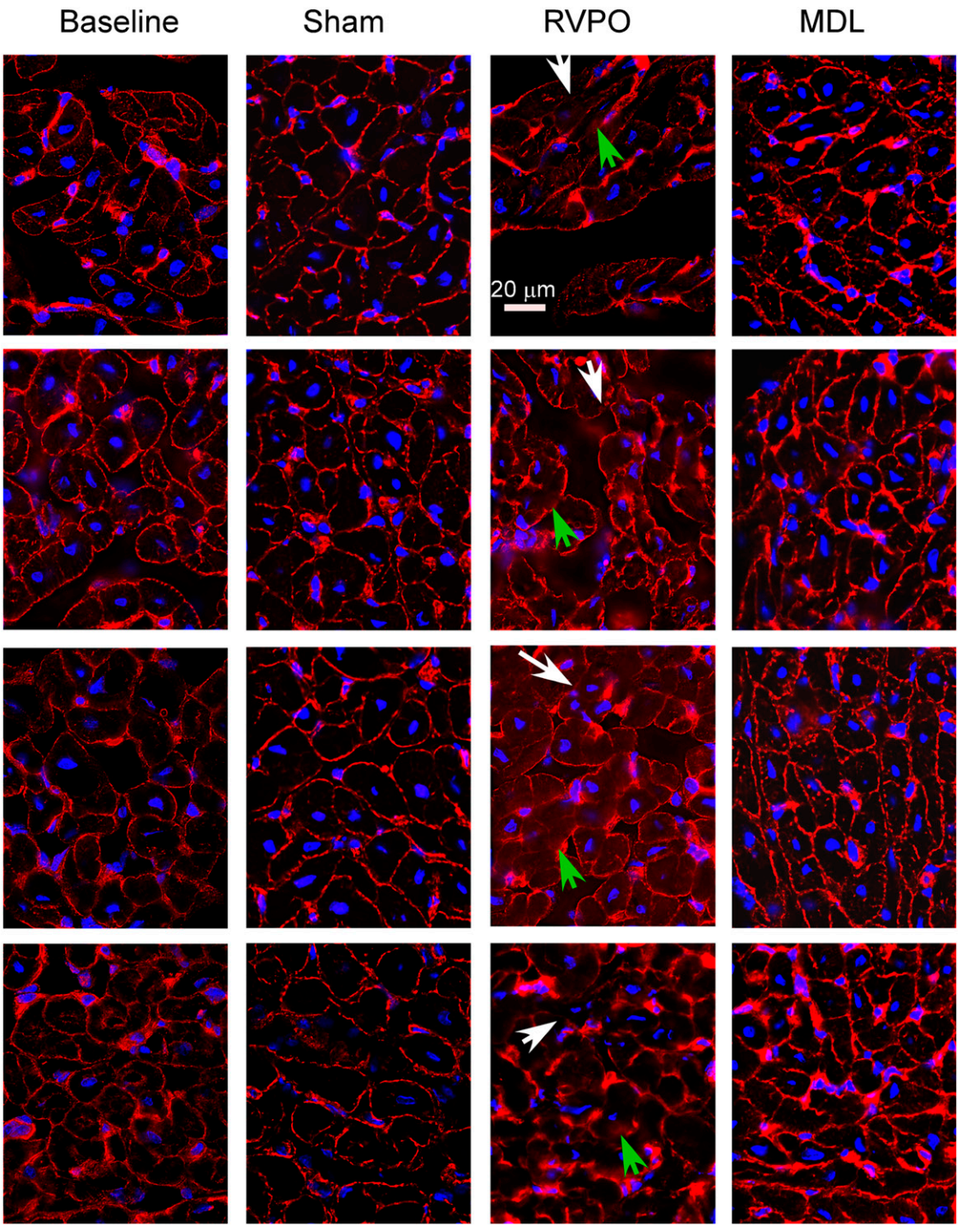

Figure 6. Talin. Representative photomicrographs were obtained from 16-μm transverse sections of the RV free wall in pigs before (Baseline) and after 2 hours of acute RVPO immunostained for talin (*red*) and with (2-(4-amidinophenyl)-1H-indole-6-carboxamidine) (DAPI) (in *blue*, for nuclei). The second biopsy was obtained from a location at least 2 cm away from the first biopsy, and in a more proximal perfusion territory, to avoid sampling a region potentially affected by the first biopsy. Under baseline conditions, the talin signal was largely localized to the cell surface. After 2 hours of acute RVPO, patchy loss of the regular signal (*white arrows*) and areas of blurring (*green arrows*) were evident. RV myocardium from pigs identically instrumented and subjected to 2 hours of anesthesia without RV pressure overload (Sham) did not exhibit any significant differences from baseline biopsies, indicating that 2 hours of anesthesia without RVPO did not cause changes in talin organization according to immunohistology. Biopsies from pigs subjected to 2 hours of RVPO but pretreated with MDL-28170 (MDL) exhibited structures more like those of Baseline and Sham than RVPO. Image sets were obtained on a Leica digital deconvolution microscope (Leica Microsystems, Buffalo Grove, IL), using a ×63 oil immersion objective (NA 1.4) with 0.5-μm z-dimension steps, and processed using constrained iterative deconvolution. Image intensity and contrast were equalized among all images. *Scale bar* = 20 μm.

Among the proteins known to be substrates for calpain are the adhesion complex proteins, including talin, integrin, α-actinin, vinculin, and focal adhesion kinase (8, 25). Focal adhesions found along the lateral subsarcolemmal surface of the myocyte, called costameres, are arranged in a two-dimensional lattice aligned parallel and transverse to the z-lines, and are believed to transmit

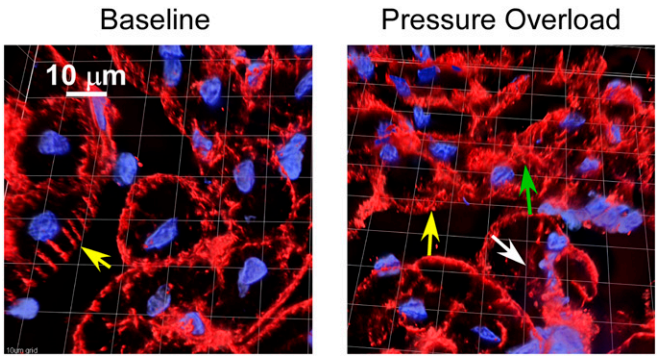

Figure 7. Talin. Detail of a three-dimensional reconstruction of a 16-μm section obtained under baseline conditions (*left*) and after 2 hours of acute RVPO (*right*), immunostained for talin (*red*) and with DAPI (in *blue*, for nuclei). Under baseline conditions, talin exhibited a regular rib-like structure coaxial with the long axis of the myocyte (*yellow arrow*, *left*). After 2 hours of acute RVPO, disruption of the regular rib-like appearance of talin occurred (*yellow arrow*, *right*), with patchy areas of signal loss (*white arrow*) and blurring (*green arrow*). The imaging technique was described in Figure 5. *Scale bar* and *grid* = 10 μm.

contractile force laterally to adjacent myocytes through attachment with the extracellular matrix (26, 27). Although the importance of lateral force transmission is less well appreciated in cardiac than in skeletal muscle, defects in the lateral transmission of force clearly contribute to some cardiomyopathies (28).

The physiological modification of proteins by calpain is critical to normal cellular development and cellular plasticity, and appears to be highly compartmentalized. Focal adhesion protein modification is an essential step in myocardial remodeling during heart failure (29), and interference with focal adhesion remodeling by calpain results in impaired contractile function in isolated myocytes (30) and even pericytes (31). In contrast to its obligatory role in normal cellular development, however, mechanical stress can activate calpain and cause an abnormal loss of talin signal in isolated muscle cells, according to other investigators (32). Because talin is among the most sensitive of the focal adhesion proteins to degradation by calpain, we used it as a surrogate for focal adhesion integrity. We found that the preservation of function was strongly related to the abundance of talin, suggesting that calpain activation and focal adhesion modification play a role in short-term contractile dysfunction from acute RVPO. Although the overall difference in talin abundance was modest, relatively small changes in major structural proteins can lead to large changes in function. For example, Supinski and Callahan found that a 30% difference in talin abundance was associated with a 30% difference in contractile function of rat diaphragm muscle after experimental endotoxemia (33). α-actinin, a major adhesion protein found predominantly at the sarcomeric z-disk that is sensitive to calpain, was similarly altered, as assessed by immunohistology, but not by Western blotting, consistent with reports by other investigators that calpain can induce major structural changes in some proteins without degrading them (34). Vinculin, another important component of focal adhesions, was similarly altered by RVPO in the present study.

In both the present and a previous study, we found that MDL-28170 preserved RV free wall contractile function through directionally favorable effects on the slope and intercept of the regional Frank–Starling relation and on regional external work at matched preload (7). In the present study, MDL-28170 exerted a significant effect to preserve the regional Frank–Starling slope, but effects on the Frank–Starling intercept and regional work did not reach statistical significance. In the previous study, effects of the drug on the Frank–Starling relation intercept and regional work were significant, whereas effects on the Frank–Starling relation slope did not achieve significance. The difference between the present and previous studies may be attributed to the duration of RV pressure overload (4 h versus 90 min, respectively) and the development of hemodynamic instability with consequently greater variability of measurements. However, it is important to note that RV free wall function makes variable contributions to overall cardiac performance depending on loading conditions. It is not surprising that RV function under conditions of RV pressure overload was more severely affected than RV function under conditions of low pulmonary vascular resistance. The impairment of RV contractile function we have identified would likely exert the greatest clinical impact when pulmonary vascular resistance cannot be completely normalized.

Although MDL-28170 is highly selective for calpain (35), we cannot absolutely exclude the possibility that MDL-28170 inhibited other proteases as well. For example, Dewachter and colleagues recently reported that RVPO induces apoptotic pathways as early as 2 hours after the onset of RVPO (36), and Mani and colleagues reported that calpain inhibition prevents programmed cell death during 24 hours of acute RVPO (37). MDL-28170 also inhibits cathepsin B, a protease that is primarily active during ischemia at low pH. We previously showed that ischemia does not play a prominent role in our model of acute RV pressure overload, but we cannot exclude the possibility that cathepsin B was activated in our model. Regardless, the disruption and loss of a major structural protein such as talin would likely contribute to impaired mechanical linkage between the sarcomere and the extracellular collagen matrix, and the preservation of mechanical integrity would in turn contribute to the maintenance of contractile function.

Conclusions

Disruption of cellular adhesion complexes may contribute to the development of RV contractile dysfunction in acute pulmonary hypertension. Calpain inhibitors such as MDL-28170 may offer a novel therapeutic strategy to mitigate the severity of RV failure in acute sustained pulmonary hypertension, a condition for which specific therapies are currently lacking.

Author disclosures are available with the text of this article at www.atsjournals.org.

Acknowledgments: Thanks go to Ron Bouchard (Denver Veterans Affairs Medical Center Imaging Core Facility) for assistance with the immunohistology studies.

References

1. Dell'Italia LJ. The right ventricle: anatomy, physiology, and clinical importance. *Curr Probl Cardiol* 1991;16:653–720.
2. Stobierska-Dzierzek B, Awad H, Michler RE. The evolving management of acute right-sided heart failure in cardiac transplant recipients. *J Am Coll Cardiol* 2001;38:923–931.
3. Greyson C, Xu Y, Cohen J, Schwartz GG. Right ventricular dysfunction persists following brief right ventricular pressure overload. *Cardiovasc Res* 1997;34:281–288.
4. Greyson C, Xu Y, Lu L, Schwartz GG. Right ventricular pressure and dilation during pressure overload determine dysfunction after pressure overload. *Am J Physiol Heart Circ Physiol* 2000;278:H1414–H1420.
5. Kerbaul F, Rondelet B, Motte S, Fesler P, Hubloue I, Ewalenko P, Naeije R, Brimioulle S. Effects of norepinephrine and dobutamine on pressure load–induced right ventricular failure. *Crit Care Med* 2004; 32:1035–1040.
6. Goll DE, Thompson VF, Li H, Wei W, Cong J. The calpain system. *Physiol Rev* 2003;83:731–801.
7. Greyson CR, Schwartz GG, Lu L, Ye S, Helmke S, Xu Y, Ahmad H. Calpain inhibition attenuates right ventricular contractile dysfunction after acute pressure overload. *J Mol Cell Cardiol* 2008;44:59–68.

8. Franco SJ, Rodgers MA, Perrin BJ, Han J, Bennin DA, Critchley DR, Huttenlocher A. Calpain-mediated proteolysis of talin regulates adhesion dynamics. *Nat Cell Biol* 2004;6:977–983.
9. Greyson C, Ahmad H, Schwartz GG, Lu L, Ye S, Xu Y. Calpain inhibition attenuates right heart failure and prevents talin degradation during acute pressure overload [abstract]. *Circulation* 2009;120:S805.
10. Greyson C, Ye S, Lu L, Xu Y, Schwartz GG, Ahmad H. Acute right ventricular pressure overload disrupts organization of the focal adhesion protein talin. *Circulation* 2010;122(Supplement):A16249. (abstract).
11. Mehdi S, Angelastro MR, Wiseman JS, Bey P. Inhibition of the proteolysis of rat erythrocyte membrane proteins by a synthetic inhibitor of calpain. *Biochem Biophys Res Commun* 1988;157:1117–1123.
12. Greyson C, Garcia J, Mayr M, Schwartz GG. Effects of inotropic stimulation on energy metabolism and systolic function of ischemic right ventricle. *Am J Physiol* 1995;268:H1821–H1828.
13. Curran-Everett D, Benos DJ. Guidelines for reporting statistics in journals published by the American Physiological Society. *Adv Physiol Educ* 2004;28:85–87.
14. Euler DE. Cardiac alternans: mechanisms and pathophysiological significance. *Cardiovasc Res* 1999;42:583–590.
15. Kostin S, Scholz D, Shimada T, Maeno Y, Mollnau H, Hein S, Schaper J. The internal and external protein scaffold of the T-tubular system in cardiomyocytes. *Cell Tissue Res* 1998;294:449–460.
16. Muhlfeld C, Coulibaly M, Dorge H, Sellin C, Liakopoulos O, Ballat C, Richter J, Schoendube F. Ultrastructure of right ventricular myocardium subjected to acute pressure load. *Thorac Cardiovasc Surg* 2004; 52:328–333.
17. Schmitto JD, Doerge H, Post H, Coulibaly M, Sellin C, Popov AF, Sossalla S, Schoendube FA. Progressive right ventricular failure is not explained by myocardial ischemia in a pig model of right ventricular pressure overload. *Eur J Cardiothorac Surg* 2009;35:229–234.
18. Colantonio DA, Van Eyk JE, Przyklenk K. Stunned peri-infarct canine myocardium is characterized by degradation of troponin T, not troponin I. *Cardiovasc Res* 2004;63:217–225.
19. Matsumura Y, Saeki E, Inoue M, Hori M, Kamada T, Kusuoka H. Inhomogeneous disappearance of myofilament-related cytoskeletal proteins in stunned myocardium of guinea pig. *Circ Res* 1996;79:447–454.
20. Papp Z, Barta J, Stienen GJ. Troponin I degradation and myocardial stunning. *Circulation* 2001;104:E157.
21. Thomas SA, Fallavollita JA, Lee TC, Feng J, Canty JM Jr. Absence of troponin I degradation or altered sarcoplasmic reticulum uptake protein expression after reversible ischemia in swine. *Circ Res* 1999;85: 446–456.
22. Tsuji T, Ohga Y, Yoshikawa Y, Sakata S, Abe T, Tabayashi N, Kobayashi S, Kohzuki H, Yoshida KI, Suga H, *et al*. Rat cardiac contractile dysfunction induced by Ca^{2+} overload: possible link to the proteolysis of alpha-fodrin. *Am J Physiol Lung Cell Mol Physiol* 2001; 281:H1286–H1294.
23. Urthaler F, Wolkowicz PE, Digerness SB, Harris KD, Walker AA. MDL-28170, a membrane-permeant calpain inhibitor, attenuates stunning and PKC epsilon proteolysis in reperfused ferret hearts. *Cardiovasc Res* 1997;35:60–67.
24. Wang YG, Benedict WJ, Huser J, Samarel AM, Blatter LA, Lipsius SL. Brief rapid pacing depresses contractile function via Ca(2+)/PKC-dependent signaling in cat ventricular myocytes. *Am J Physiol Lung Cell Mol Physiol* 2001;280:H90–H98.
25. Chan KT, Bennin DA, Huttenlocher A. Regulation of adhesion dynamics by calpain-mediated proteolysis of focal adhesion kinase (FAK). *J Biol Chem* 2010;285:11418–11426.
26. Anastasi G, Cutroneo G, Gaeta R, Di Mauro D, Arco A, Consolo A, Santoro G, Trimarchi F, Favaloro A. Dystrophin–glycoprotein complex and vinculin–talin–integrin system in human adult cardiac muscle. *Int J Mol Med* 2009;23:149–159.
27. Danowski BA, Imanaka-Yoshida K, Sanger JM, Sanger JW. Costameres are sites of force transmission to the substratum in adult rat cardiomyocytes. *J Cell Biol* 1992;118:1411–1420.
28. Heydemann A, McNally EM. Consequences of disrupting the dystrophin–sarcoglycan complex in cardiac and skeletal myopathy. *Trends Cardiovasc Med* 2007;17:55–59.
29. Brancaccio M, Hirsch E, Notte A, Selvetella G, Lembo G, Tarone G. Integrin signalling: the tug-of-war in heart hypertrophy. *Cardiovasc Res* 2006;70:422–433.
30. Imanaka-Yoshida K, Enomoto-Iwamoto M, Yoshida T, Sakakura T. Vinculin, talin, integrin alpha6beta1 and laminin can serve as components of attachment complex mediating contraction force transmission from cardiomyocytes to extracellular matrix. *Cell Motil Cytoskeleton* 1999;42:1–11.
31. Kotecki M, Zeiger AS, Van VKJ, Herman IM. Calpain- and talin-dependent control of microvascular pericyte contractility and cellular stiffness. *Microvasc Res* 2010;80:339–348.
32. Grossi A, Karlsson AH, Lawson MA. Mechanical stimulation of C2C12 cells increases M-calpain expression, focal adhesion plaque protein degradation. *Cell Biol Int* 2008;32:615–622.
33. Supinski GS, Callahan LA. Calpain activation contributes to endotoxin-induced diaphragmatic dysfunction. *Am J Respir Cell Mol Biol* 2010; 42:80–87.
34. Goll DE, Dayton WR, Singh I, Robson RM. Studies of the alpha-actinin/actin interaction in the z-disk by using calpain. *J Biol Chem* 1991;266: 8501–8510.
35. Mehdi S. Cell-penetrating inhibitors of calpain. *Trends Biochem Sci* 1991;16:150–153.
36. Dewachter C, Dewachter L, Rondelet B, Fesler P, Brimioulle S, Kerbaul F, Naeije R. Activation of apoptotic pathways in experimental acute afterload-induced right ventricular failure. *Crit Care Med* 2010;38: 1405–1413.
37. Mani SK, Shiraishi H, Balasubramanian S, Yamane K, Chellaiah M, Cooper G, Banik N, Zile MR, Kuppuswamy D. *In vivo* administration of calpeptin attenuates calpain activation and cardiomyocyte loss in pressure-overloaded feline myocardium. *Am J Physiol Lung Cell Mol Physiol* 2008;295:H314–H326.